Delft University of Technology

Polarimetric diversity in reference-free amplitude-based Wi-Fi sensing

Bongioanni, Carlo; Colone, Fabiola; Di Seglio, Marco; Filippini, Francesca; Fioranelli, Francesco

DOI
10.1109/RadarConf2458775.2024.10548886

Publication date
2024

Published in
RadarConf 2024 - 2024 IEEE Radar Conference, Proceedings

Citation (APA)
Bongioanni, C., Colone, F., Di Seglio, M., Filippini, F., & Fioranelli, F. (2024). Polarimetric diversity in reference-free amplitude-based Wi-Fi sensing. In *RadarConf 2024 - 2024 IEEE Radar Conference, Proceedings* (Proceedings of the IEEE Radar Conference). IEEE. https://doi.org/10.1109/RadarConf2458775.2024.10548886

Important note
To cite this publication, please use the final published version (if applicable). Please check the document version above.

Copyright
Other than for strictly personal use, it is not permitted to download, forward or distribute the text or part of it, without the consent of the author(s) and/or copyright holder(s), unless the work is under an open content license such as Creative Commons.

Takedown policy
Please contact us and provide details if you believe this document breaches copyrights. We will remove access to the work immediately and investigate your claim.

This work is downloaded from Delft University of Technology.
For technical reasons the number of authors shown on this cover page is limited to a maximum of 10.

Green Open Access added to TU Delft Institutional Repository

'You share, we take care!' - Taverne project

https://www.openaccess.nl/en/you-share-we-take-care

Otherwise as indicated in the copyright section: the publisher
is the copyright holder of this work and the author uses the
Dutch legislation to make this work public.

Polarimetric diversity in reference-free amplitude-based Wi-Fi sensing

Carlo Bongioanni[1], Fabiola Colone[2], Marco Di Seglio[3], Francesca Filippini[2], Francesco Fioranelli[4]

[1]School of Advanced Defence Studies, Rome, Italy
{carlo.bongioanni@ssuos.difesa.it}
[2]Dept. of Information Engineering, Electronics and Telecommunications, Sapienza University of Rome, Italy
{fabiola.colone, francesca.filippini}@uniroma1.it
[3]Dept. of Cognitive Procedures, Fraunhofer Institute for High Frequency Physics and Radar Techniques (FHR), Wachtberg, Germany{marco.di.seglio@fhr.fraunhofer.de}
[4]Microwave Sensing Signals & Systems (MS3) Group, TU Delft, Delft, The Netherlands
{f.fioranelli@tudelft.nl}

Abstract — **Passive sensing exploiting Wi-Fi as an illuminator of opportunity has attracted considerable interest for the ubiquitous presence of Wi-Fi systems in many environments, and the relative low cost & complexity of related passive solutions. In this paper, we consider a reference-free, amplitude-based sensing strategy exploiting Wi-Fi signals of opportunity and we investigate the potential advantage conveyed by the use of polarimetric diversity on receive. Specifically, we exploit the data collected by a dual-pol receiver to experimentally demonstrate that the joint availability of the signals collected by differently polarized antennas (H and V) could remarkably enhance the detection performance of the resulting Wi-Fi sensor, even if based on such a simple and cost-effective reference-free sensing approach. Moreover, we analyze the characteristics of the target signatures extracted by the considered amplitude-based approach for either single and dual-pol receivers, in order to investigate their suitability for detecting and recognizing different human movements, in view of future applications for automatic classification.**

Keywords — Wi-Fi sensing, passive sensing, amplitude-based sensing, forward scatter radar, polarimetric radar, feature extraction.

I. INTRODUCTION

The widespread proliferation of Wi-Fi Access Points (APs) in recent years has made them excellent candidates for illuminators to be exploited parasitically in passive radar techniques, and cooperatively in integrated sensing and communication (ISAC) systems. Hence, not surprisingly, several studies in the literature have demonstrated the suitability of Wi-Fi signals [1] for passive sensing, i.e., without the usage of a dedicated transmitter with the related issues of costs, power consumption, and above all spectral occupancy, in scenarios where the electromagnetic spectrum is increasingly congested. Applications include detection and localization of ground vehicles and small unmanned aerial vehicles (UAVs) in outdoor scenarios, as well as personnel in outdoor and indoor environments [2]-[6]. Another key aspect of Wi-Fi sensing that has drawn considerable attention is the human activity recognition capability for healthcare and contactless vital signs monitoring [11]-[13].However, most Wi-Fi based sensors rely on Channel State Information-based approaches or on classical radar techniques. In both cases, complex valued signals are considered to implement the required, often adaptive, signal processing techniques in order to mitigate the interference and focus the target echo energy. The use of coherent approaches that heavily rely on the phase stability at the receiver sets strict requirements in terms of hardware, which might increase the cost of the sensing solution.

In contrast, the use of non-coherent sensors, namely sensors that only exploit the amplitude of the received signals, has the potential to relax the requirements on the receiver design, thus enabling low-cost Wi-Fi sensing solutions [10]-[13]. In this paper, we consider the Interference Doppler Processing (IDP) technique that was recently proposed in [10] for Wi-Fi sensing. The basic idea is the same as that used in forward scatter radar (FSR) systems [11], but adapted to the case of a pulsed signal exploiting amplitude modulated waveforms. In [10] it was demonstrated how IDP could detect the presence of moving targets by extracting the amplitude modulation induced by the target echo on the main Wi-Fi signal generated by the AP. This is obtained by implementing a very simple receiver architecture both in terms of required hardware and signal processing stages.

To perform a further step in our understanding of the Wi-Fi sensing based on IDP, this work explores the information conveyed by different polarimetric channels on receive. To this purpose, we use the experimental data simultaneously received at the V-polarized and H-polarized antennas connected to a dual channel receiver. Different tests are performed in different scenarios with different targets, namely a bicyclist and a cooperative small UAV. It is shown that the different polarimetric channels highlight different information of the target's signatures, and that this information can be exploited in a joint manner to enhance the detection performance.

In addition, we investigate the potential of the resulting system in terms of classification capability. Specifically, first we look at the impact of the target movements on the direct Wi-Fi signal amplitude, by exploiting experimental data featuring a person performing different arm and body movements. The analysis shows that each movement modulates the amplitude in a unique and remarkably stable way, hence revealing the possibility of a human activity classification even using such a simple sensing approach. Moreover, we show that the target signatures collected at the two polarimetric channels have diverse characteristics and we explore the possibility to jointly exploit these signatures in order to improve the discrimination capability among different body movements. To this aim, we perform a

2024 IEEE Radar Conference (RadarConf24) | 979-8-3503-2920-9/24/$31.00 ©2024 IEEE | DOI: 10.1109/RADARCONF2458775.2024.10548886

978-1-7281-8942-0/20/$31.00 ©2020 IEEE

Authorized licensed use limited to: TU Delft Library. Downloaded on February 05,2025 at 12:57:47 UTC from IEEE Xplore. Restrictions apply.

clustering of the data according to a two-component Principal Component Analysis (PCA) when using the polarimetric channels, both separately and jointly. The analysis shows that a better separation between the clusters and a better cluster variance is achieved with the dual-pol approach, compared to the case of using a single polarization on its own.

The rest of the paper is organized as follows. Section II discusses the proposed IDP approach. Section III introduces the setup and experimental data collection, together with results generated using the IDP processing. Section IV presents the experimental setup, data collection process and the results for the classification of human activities. Finally, Section V concludes the paper.

II. REFERENCE-FREE AMPLITUDE-BASED SENSING

Aiming at low cost sensing solutions, the use of non-coherent radar sensors has been investigated in the literature, such as those based on the FSR principle [11][12]. The application of this principle to the case of Wi-Fi sensing has led to the definition of the Interference Doppler Processing approach [10], which is briefly summarized in the following.

The IDP basically extracts the amplitude modulation that the echo from a moving target induces at the receiver on the direct signal coming from the Wi-Fi AP. This is obtained by means of a very simple processing scheme sketched in Figure 1.

Let $x_p(l), l = 0, \dots, N_p - 1$ be the discrete version of the complex baseband signal received for the pth Wi-Fi packet emitted by the AP, composed by N_p samples. First, the packet energy is extracted, i.e., the square modulus of the signal is evaluated, followed by an energy detector at packet level, over a portion of N samples:

$$z(p) = \sum_{l=0}^{N-1} \left|x_p(l)\right|^2 \qquad (1)$$

The authors in [10] have demonstrated that selecting N so that to limit the above summation to time-invariant and data-independent portions of the Wi-Fi packet, e.g., the PHY Preamble, is the most suitable solution in order to maximize the capability to distinguish the target induced amplitude modulation from the inherent amplitude modulation of the exploited OFDM waveforms.

Once this stage has been performed, the sequence of samples $z(p), p = 0, \dots, P - 1$, undergoes a DC removal stage, aimed at removing the strongest stationary scene components, above all the direct signal from the AP:

$$\underline{z}(p) = z(p) - z_{DC}(p) \qquad (2)$$

where $z_{DC}(p)$ represents the average value of $z(p)$, evaluated over an appropriate time window T_{DC} around the current sample.

Finally, $\underline{z}(p)$ undergoes a time-frequency analysis that provides as output the typical spectrogram, where the presence of a target is detected via its Doppler signature. Specifically, assuming that the packet emission rate is constant over time, a short-time Fourier transform (STFT) can be implemented that operates against partially overlapped batches of T_{STFT} seconds each, corresponding to P_{STFT} samples:

$$w(m) = \sum_{p=0}^{P_{STFT}-1} h(p)\underline{z}(p_0 + p)e^{-j2\pi\frac{mp}{P_{STFT}}} \qquad (3)$$

where p_0 is the first packet of the considered batch and $h(p)$ is an appropriate weighting function, employed to control the Doppler sidelobes level.

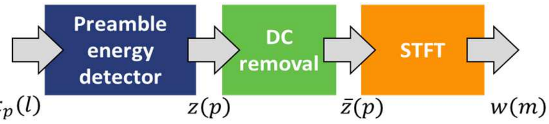

Figure 1. Processing blocks of the single-polarimetric Interference Doppler Processing (IDP) scheme.

III. DETECTION RESULTS USING DIFFERENT POLARIZATIONS

In this section we investigate the use of the IDP approach in a dual-pol receiver with the aim of understanding the potential advantages in terms of target detection capability.

A. *Experimental setup*

A dedicated campaign was conducted in a private outdoor premise, shown in Figure 2(a), where a commercial Wi-Fi AP (TP-Link Archer VR600 AC1600) was employed to transmit signals according to the IEEE 802.11ac Standard [1] at a carrier frequency of 5.18 GHz on channel 36 of the Wi-Fi band. This device was connected to a transmitting directive antenna (Ubiquiti UMA-D), with V polarization (see the red square at the bottom-right corner of Figure 2(a)).

(a)

(b)

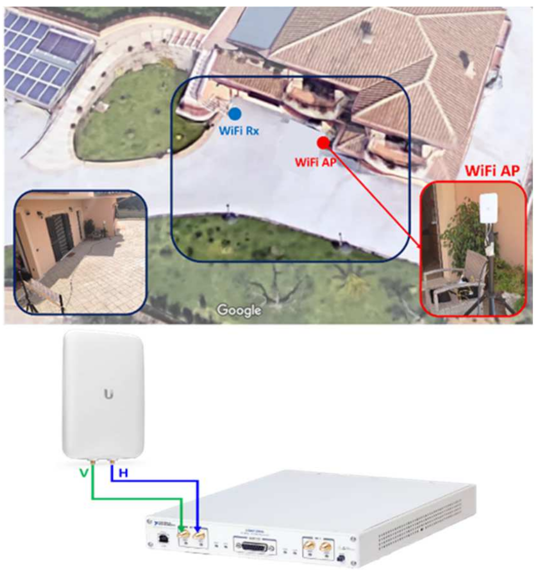

Figure 2. Experimental setup for the 1st measurement campaign: (a) acquisition geometry; (b) dual-polarimetric antenna and USRP used as receiver.

A dual-polarimetric antenna (Ubiquiti UMA-D) was employed at the receive side, with H (Cross-polarization configuration) and V (Co-polarization configuration) outputs connected to a National Instruments NI USRP-2955 board shown in Figure 2(b), set to a Nyquist sampling frequency of 20 MHz. The TX-RX setup is characterized by extreme

Authorized licensed use limited to: TU Delft Library. Downloaded on February 05,2025 at 12:57:47 UTC from IEEE Xplore. Restrictions apply.

bistatic angles. Exploiting this setup, two tests were conducted. In test #1 a small drone acting as a cooperative target was flown across the TX-RX baseline. In test #2 a person acted as a cooperative target riding a bicycle across the TX-RX baseline.

B. Test #1: small drone

This test has been conducted to investigate the detection capabilities, exploiting different polarimetric channels for small RCS targets. To this purpose, a small drone (DJI Mavic Pro) was exploited as a cooperative target. Specifically, in the performed test, the drone was flown close to the TX-RX baseline along an orthogonal trajectory and moved away. This pattern has been repeated two times. The first time the drone was close to the TX-RX baseline, it stopped for about 7 seconds while rotating on itself, and then moved away losing and regaining altitude due to some piloting uncertainty. The second time the drone was close to the TX-RX baseline, it stopped for about 5 seconds while rotating on itself, and then moved away in a more regular trajectory than the first time. The result with the co-pol configuration, namely applying the IDP on the data collected at the V channel, has been already shown and discussed in [14], however in this work we investigate the difference between adopting different polarimetric channels on receive.

To this purpose, Figure 3 reports the spectrogram obtained at the output of the IDP processing scheme for both the V-pol and the H-pol channels. The IDP operates with a STFT window of $T_{STFT} = 0.5$ s and a cancellation interval of 0.5 s; both spectrograms have been scaled to the estimated background level in order to show a better comparison between the two polarizations.

In both reported cases the target signature can be well recognized along its entire trajectory. However, some key differences can be noted. For instance, some portions of the target signature are characterized by a higher level depending on which polarimetric channel is exploited.

This can be easily verified when comparing the output for the V-pol (Figure 3(a)) and the H-pol (Figure 3(b)) data in the time interval [5,15] s. In fact, the V-pol data shows a higher level for the target signature. The opposite happens in the time interval [25,32] s, where the highest level is obtained when using the H-pol data. However, in such interval the data from the V-pol channel shows a continuous signature compared to the H-pol data, meaning that the target could be more reliably detected across its trajectory. Finally, in the interval [45,55] s the spectrogram for the data from the H-pol channel shows a higher level as well as a more continuous target signature.

These results clearly suggest that the joint exploitation of the two polarimetric channels enables to capture different information of the target signature, which can lead to a better performance in the detection of the small UAV while still keeping limited the complexity of the sensor.

C. Test #2: bicyclist

A similar test has been conducted on a larger target, represented by a cooperative human riding a bicycle. Specifically, in the test performed, the target starts close to the TX-RX baseline, crossing it while it moves away. The spectrogram obtained for the two polarimetric channels at the output of the IDP have been reported in Figure 4, using the same processing parameters adopted in the previous test.

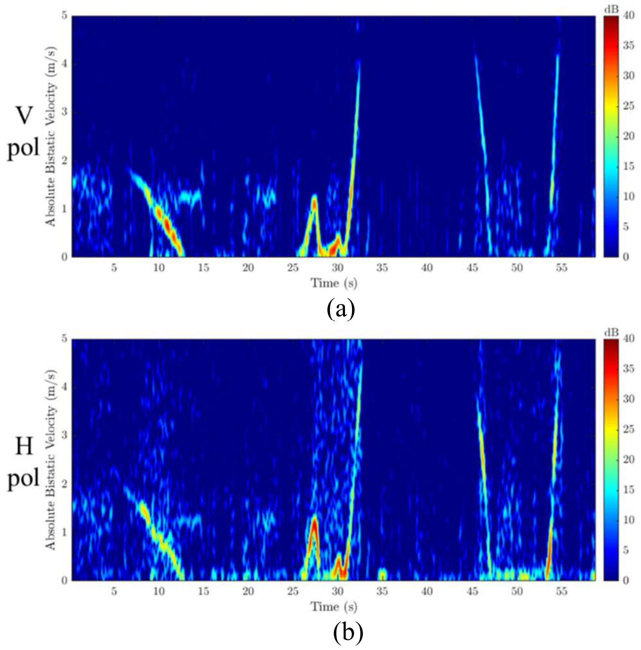

Figure 3. Output spectrograms obtained for the experimental test with the small drone, for the two pol channels, i.e., V (a) and H (b).

As it can be seen, in both spectrograms obtained from the V-pol channel (Figure 4(a)) and the H-pol channel (Figure 4(b)), the target signature can be easily discriminated from the background up to 5s, when the bicyclist leaves the beam of the TX antenna.

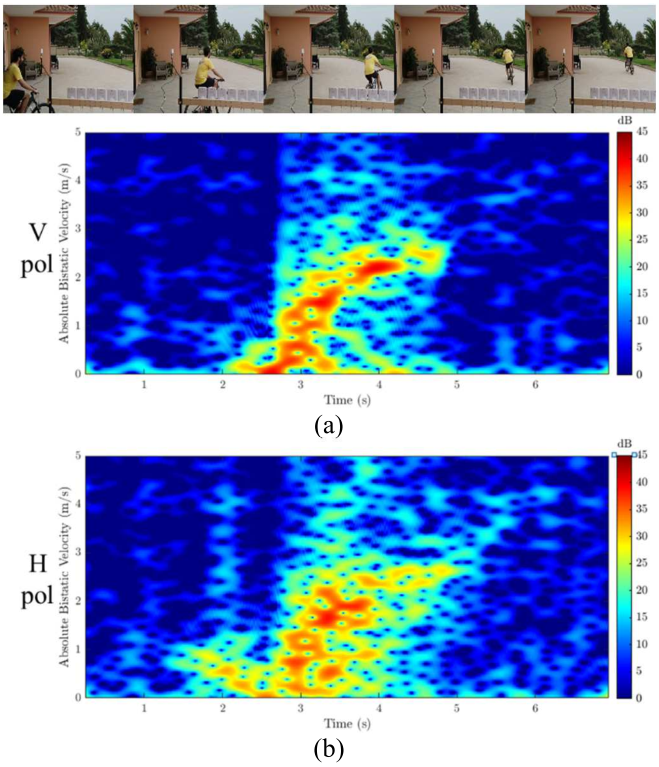

Figure 4 Test with bicycle: video frames of the exploited test (top) and output spectrograms obtained for the two pol channels, i.e., V (a) and H (b).

However, by exploiting the data from the H-pol channel, an early detection of the target could be achieved compared to the other channel (i.e., about 1s earlier), although the target signature is affected by a larger spread along the bistatic

Authorized licensed use limited to: TU Delft Library. Downloaded on February 05,2025 at 12:57:47 UTC from IEEE Xplore. Restrictions apply.

velocity that possibly reveals an increased sensitivity to the motion of the bicyclist body parts. The use of the data from the V-pol channel, instead, allows for a finer target signature characterization in the bistatic velocity domain that might result in a better translational velocity estimation. Again, the reported results show the potential benefits of employing both polarimetric channels within the context of the IDP approach, as they may provide complementary information on the surveyed scene.

IV. POLARIMETRIC FEATURES OF HUMAN ACTIVITIES

The work showed until now has focused on analysing the use of different polarimetric channels for detection purposes when an IDP approach is used. This section focuses on the use of different polarimetric channels to characterize the target-induced amplitude modulation for classification purposes. For this, the IDP processing chain of Figure 1 is limited to its first stage as we analyze and compare the output of the energy detector.

A. *Experimental setup*

Another experimental campaign was performed in a different private outdoor premise, shown in Figure 5(a), with the aim of analyzing the potentialities of an amplitude-based approach such as the IDP in terms of human movements discrimination and the impact of the receiver polarization on the target-induced amplitude modulation.

The experimental setup, sketched in Figure 5(b), was similar to the setup described in section III. The same Wi-Fi AP and directive antenna were used as transmitter, and the NI USRP with dual-polarized antennas were used at the receiver in a FSR geometry with respect to the transmitter (see the yellow square in Figure 5(a)). The distance between the transmitting antenna and the receiving antenna in FSR configuration (baseline) was about 8.4 m.

(a)

(b)

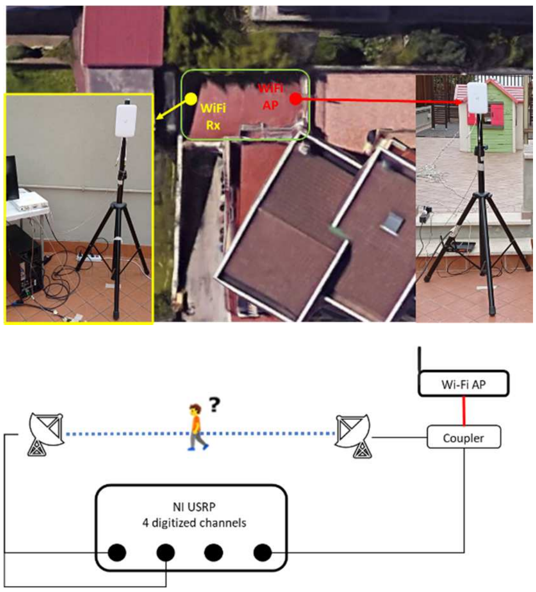

Figure 5. Experimental setup for the 2nd measurement campaign: (a) acquisition geometry, (b) sketch of the setup and components.

In this case, a person acted as a cooperative target standing along the baseline at about 4 m from the receiving antenna, facing the receiver and performing different movements, considered as potential classes in a classification problem. These were:

1. Class #1: extend and bend arms in the lateral direction while standing.
2. Class #2: extend and bend arms in the upward direction above the head while standing.
3. Class #3: extend and bend arms in the frontal direction while standing.
4. Class #4: squatting down and coming back up (with no specific indications given as to the movement of the arms while squatting).
5. Class #5: lateral raise of arms while standing, similar to performing a typical "jumping jack" exercise, but without jumping.
6. Class #6: bending with the full body forward towards the radar and backward (similar to a bowing movement).
7. Class #7: bending with the full body on the right and left side.

Visual examples of three of the performed movements are reported in Figure 6. For each of the aforementioned movements, a sequence consisting of $K = 6$ repetitions of such movement were collected, and the participants were asked to take a small pause between the repetitions. For simplicity, a metronome set to 50 bpm was used to provide the different participants with an approximate timing reference, aimed at having acquisitions as synchronous as possible between different people for this preliminary study.

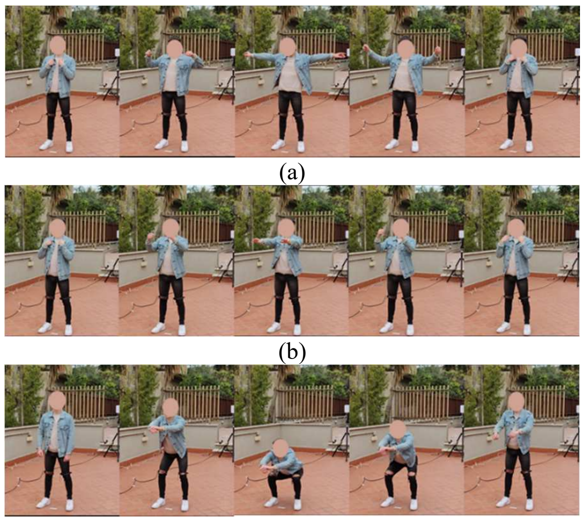

(a)

(b)

(c)

Figure 6. Visual example of performed movements: (a) lateral extension of the arms; (b) frontal extension of the arms; (c) squat.

A. *Polarimetric signatures*

An example of the amplitude modulation induced by the target movements on the received signal can be seen in Figure 7, where 3 repetitions for class #1 (Figure 7(a)), #3 (Figure 7(b)) and #4 (Figure 7Figure 7(c)), from the H-pol channel, are reported. Due to the non-constant packet emission rate in Wi-Fi transmissions, the output of the energy detector has been resampled over a uniform time grid, in order to simplify the comparison of different results for different tests and classes. By comparing the sub-figures it is possible to note that each movement induces a rather different amplitude

Authorized licensed use limited to: TU Delft Library. Downloaded on February 05,2025 at 12:57:47 UTC from IEEE Xplore. Restrictions apply.

modulation. A similar effect can be noticed when analyzing the amplitude signature obtained from the V-pol channel in Figure 8. These results highlight the fact that, in both polarimetric channels, different movements produce unique amplitude modulations, which might be exploited to classify them. In this work we resort to a Principal Component Analysis (PCA) with two components, in order to achieve a clustering of the features extracted from the different classes. Specifically, the amplitude signature is collected separately for each repetition of the different movements, and stored row-wise into a data matrix with dimensions $7K \times L$, where $K = 6$ is the number of repetitions available for each class, and L is the number of samples. The obtained data matrix is then exploited for the PCA.

The output of the PCA applied in the data collected from the H-pol channel is reported in Figure 9(a), where it can be seen that only class #1 and class #4 are effectively well separated, whereas the other classes cannot be distinguished from each other since their feature samples are overlapping. A similar result is achieved when exploiting the data collected from the V-pol channel. In fact, the output of the PCA reported in Figure 9(b) shows a better clustering performance, meaning that in this case the classes do present more differences between each other. However, despite achieving a better clustering performance compared to the other polarimetric channel, the feature samples of class #1, #3, #4 are still in part overlapped, whereas class #2 and #7 are overlapped.

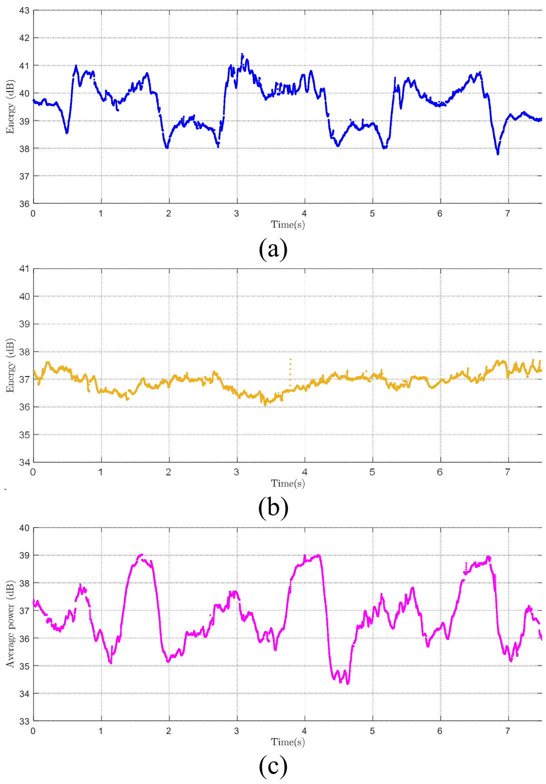

Figure 7. Energy signatures from the H polarimetric channel for class #1 (a), class #3 (b) and class #4 (c), where three repetitions of the movement for each class are shown.

In order to achieve a better clustering performance, the data from both polarimetric channels can be jointly exploited. In fact, since the two polarimetric channels highlight different information on the target movements, as it can be seen by comparing Figure 7 and Figure 8, their joint exploitation can potentially lead to a better clustering performance.

To do so, we first separate each repetition of each movement for both polarimetric channels, as previously done for the single polarization cases, so to achieve K vectors with length L for each class. After the movement repetitions are separated for each polarimetric channel, the amplitude signature segments from the V-pol channel are appended to the corresponding ones from the H-pol channel, so that for each class we have K vectors of length $2L$. It is important to note that the data are acquired via dual-channel receiver, thus the data for the two polarimetric channels are time-synchronous.

Subsequently, we collect all the repetition of each class in a data matrix with dimensions $7K \times 2L$ that is then exploited for the two components PCA, whose output is shown in Figure 10. This result shows that all classes are effectively separated in the 2D feature space, also achieving a smaller cluster variance. Such results show that a good classification performance could in this case be achieved by exploiting simple classification algorithm, e.g., k-nearest neighbors, as the feature samples are already well clustered and separated.

However, more sophisticated classification approaches should be exploited in real-world scenarios in order to take into account the speed variance in performing each movement as well as other non-ideal effects. Nevertheless, the reported analysis allowed to demonstrate the potentialities of the proposed amplitude-based Wi-Fi sensor for classification purposes, and the advantages conveyed by the availability of different polarimetric channels on receive.

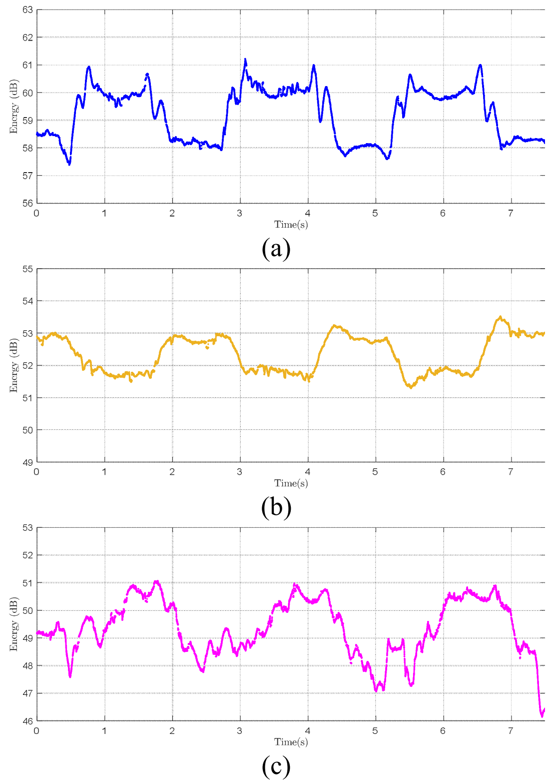

Figure 8. Energy signatures from the V polarimetric channel for class #1 (a), class #3 (b) and class #4 (c), where three repetitions of the movement for each class are shown.

Authorized licensed use limited to: TU Delft Library. Downloaded on February 05,2025 at 12:57:47 UTC from IEEE Xplore. Restrictions apply.

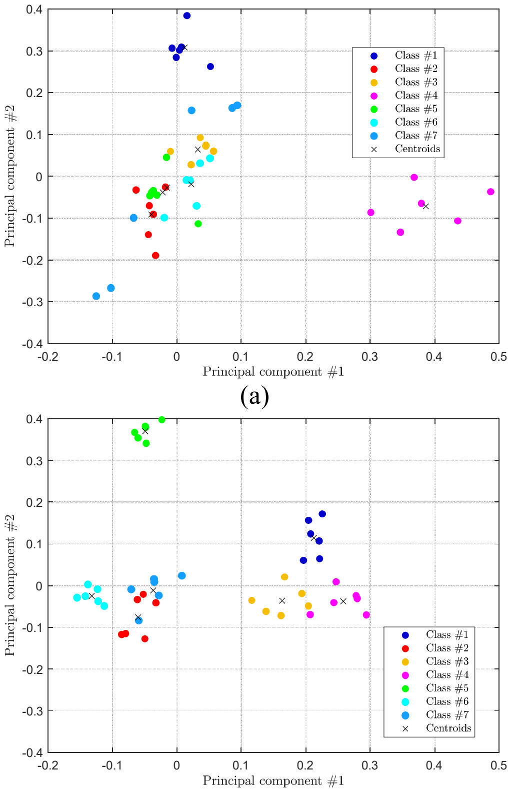

(a)

(b)

Figure 9. Output of the PCA with two features when applied on the data acquired from the H polarimetric channel (a), and on the data acquired from the V polarimetric channel (b).

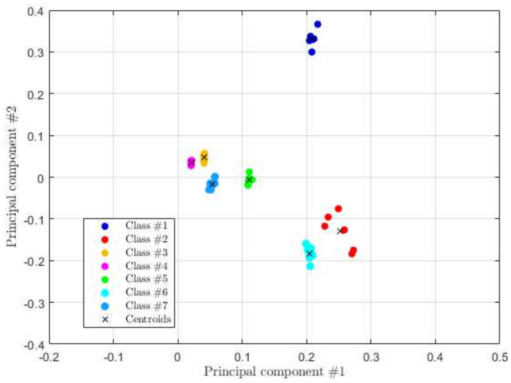

Figure 10. Output of the PCA with two features applied on the joint data from both polarimetric channels.

V. CONCLUSION

In this paper we experimentally investigated the potentialities of a reference-free, amplitude-based Wi-Fi sensor when equipped with two orthogonally polarized channels on receive. Specifically, we have shown that the joint availability of the signals collected by differently polarized antennas (H and V) could remarkably enhance the detection performance of the resulting Wi-Fi sensor, even if based on such a simple and cost-effective reference-free sensing approach. Moreover, the analysis of the target amplitude signatures extracted for either single and dual-pol receivers has preliminary shown their suitability for recognizing different human movements. In particular, the provided results have shown that, through the use of a simple PCA feature extraction, the joint exploitation of the polarimetric information results in better clustering of samples related to different human movements. This might lead to a better classification performance to be investigated in the following steps of this work.

VI. AKNOWLEDGMENT

This work was partially supported by the European Union under the Italian National Recovery and Resilience Plan (NRRP) of NextGenerationEU, partnership on "Telecommunications of the Future" (PE00000001 - program "RESTART", CUP B53C22004050001).

REFERENCES

[1] Wireless LAN Medium Access Control (MAC) and physical Layer (PHY) Specifications, IEEE Std. 802.11, 2016.

[2] F. Colone, P. Falcone, C. Bongioanni and P. Lombardo, "WiFi-Based Passive Bistatic Radar: Data Processing Schemes and Experimental Results", in *IEEE Transactions on Aerospace and Electronic Systems*, vol. 48, no. 2, pp. 1061-1079, April 2012.

[3] K. Chetty, G. E. Smith and K. Woodbridge, "Through-the-Wall Sensing of Personnel Using Passive Bistatic WiFi Radar at Standoff Distances", in *IEEE Transactions on Geoscience and Remote Sensing*, vol. 50, no. 4, pp. 1218-1226, April 2012.

[4] H. Sun, L. G. Chia and S. G. Razul, "Through-Wall Human Sensing With WiFi Passive Radar", in *IEEE Transactions on Aerospace and Electronic Systems*, vol. 57, no. 4, pp. 2135-2148, Aug. 2021.

[5] F. Colone, F. Filippini, M. Di Seglio and K. Chetty, "On the Use of Reciprocal Filter Against WiFi Packets for Passive Radar", in *IEEE Transactions on Aerospace and Electronic Systems*, vol. 58, no. 4, pp. 2746-2761, Aug. 2022.

[6] M. Di Seglio, F. Filippini, C. Bongioanni, and F. Colone, " Reference-free WiFi PHY Preamble based Passive Radar for Human Sensing", *2022 IET International Radar Conference,* Edinburgh, UK, 2022.

[7] B. Tan, Q. Chen, K. Chetty, K. Woodbridge, W. Li and R. Piechocki, "Exploiting WiFi Channel State Information for Residential Healthcare Informatics", in *IEEE Communications Magazine*, vol. 56, no. 5, pp. 130-137, May 2018.

[8] J. Liu, Y. Chen, Y. Wang, X. Chen, J. Cheng and J. Yang, "Monitoring Vital Signs and Postures During Sleep Using WiFi Signals". in *IEEE Internet of Things Journal*, vol. 5, no. 3, pp. 2071-2084, June 2018.

[9] C. Wu, F. Zhang, Y. Hu and K. J. R. Liu, "GaitWay: Monitoring and Recognizing Gait Speed Through the Walls", in *IEEE Transactions on Mobile Computing*, vol. 20, no. 6, pp. 2186-2199, 1 June 2021.

[10] F. Colone, *et al.*, "Reference-free Amplitude-Based WiFi Passive Sensing", in *IEEE Transactions on Aerospace and Electronic Systems,* vol. 59, no. 5, pp. 6432-6451, Oct. 2023.

[11] M. Cherniakov, "Basic principles of forward-scattering radars, " in Bistatic Radar: Principles and Practice: Part III. New York, NY, USA: Wiley, 2007.

[12] M. Gashinova, L. Daniel, A. Myakinkov, and M. Cherniakov, " Forward scatter radar", in Novel Radar Techniques and Applications Volume 1: Real Aperture Array Radar, Imaging Radar, and Passive and Multistatic Radar. Raleigh, NC, USA: SciTech, 2017, ch. 13, pp. 563–619.

[13] F. Colone, "DVB-T-Based Passive Forward Scatter Radar: Inherent Limitations and Enabling Solutions", in *IEEE Transactions on Aerospace and Electronic Systems*, vol. 57, no. 2, pp. 1084-1104, April 2021.

[14] F. Filippini, M. Di Seglio, C. Bongioanni, P. V. Brennan and F. Colone, "OFDM based WiFi Passive Sensing: a reference-free non-coherent approach", 2023 IEEE Radar Conference (RadarConf23), San Antonio, TX, USA, 2023, pp. 1-6, doi: 10.1109/RadarConf2351548.2023.10149694.

Authorized licensed use limited to: TU Delft Library. Downloaded on February 05,2025 at 12:57:47 UTC from IEEE Xplore. Restrictions apply.